

# Highly Water-Stable PEDOT:PSS Composite Electrode Decorated with Polyvinylpyrrolidone and Carbon Nanotubes for Sensitive Detection of Eugenol

Zifei Wang<sup>1</sup>, Yuanyuan Yao<sup>1</sup>, Hui Zhang<sup>1</sup>, Jie Zhang<sup>1</sup>, Wanchuan Ding<sup>1</sup>, Zhen Liu<sup>1</sup>, Jingkun Xu<sup>1,\*</sup>, and Yangping Wen<sup>2,\*</sup>

<sup>1</sup> School of Pharmacy, Jiangxi Science and Technology Normal University, Nanchang 330013, PR China

<sup>2</sup> Key Laboratory of Applied Chemistry, Jiangxi Agricultural University, Nanchang 330045, PR China

\*E-mail: [xujingkun@tsinghua.org.cn](mailto:xujingkun@tsinghua.org.cn); [wenyangping1980@gmail.com](mailto:wenyangping1980@gmail.com)

Received: 4 June 2015 / Accepted: 28 June 2015 / Published: 28 July 2015

---

A high-performance poly(3,4-ethylenedioxythiophene):poly(styrene-sulfonate) (PEDOT:PSS) composite electrode with high water stability, which has become a crucial problem how to solve the potential application of PEDOT:PSS film electrode in water, for the simple and sensitive voltammetric determination of eugenol in food samples was successfully fabricated. Chitosan, hydroxyethyl cellulose (HEC), and polyvinylpyrrolidone (PVP) as binders and stabilizers were respectively incorporated into a commercially available aqueous PEDOT:PSS dispersion to address the above-mentioned issues by studying flexibility, soaking stability, adhesion stability, cycle stability, and conducting property. Meanwhile, a commercially available aqueous single-walled carbon nanotube (SWCNTs) dispersion was also introduced to enhance sensing performance of PEDOT:PSS film electrode. PEDOT:PSS-SWCNTs-PVP electrode exhibited best electrode stability in water and electrocatalytic ability toward eugenol compared with PEDOT:PSS-SWCNTs-chitosan electrode and PEDOT:PSS-SWCNTs-HEC electrode. The as-fabricated electrochemical eugenol sensor based on PEDOT:PSS-SWCNTs-PVP exhibited wide linear range from 0.15 to 122.4  $\mu\text{M}$  with a low detection limit of 0.048  $\mu\text{M}$  ( $S/N = 3$ ), high sensitivity, pronounced stability, good selectivity and practicability. Satisfactory results indicated that PEDOT:PSS-SWCNTs-PVP with high electrode stability in water will provide a promising platform for the potential application in electrochemical devices like chemo/bio sensors, supercapacitors, fuel cells, and batteries.

---

**Keywords:** PEDOT:PSS; Electrochemical sensor; Polyvinylpyrrolidone; Water stability; Eugenol

## 1. INTRODUCTION

Eugenol, the major phenolic component of clove oil, was mainly found in plant products, for instance, cloves, bay leaves and allspice [1-2]. In addition, it is widely used as a flavoring agent and

fragrance in food and cosmetic industries [3]. Furthermore, various biological activities, such as anti-oxidation, anti-inflammatory, and anti-bacterial activity, has been demonstrated to against gram positive and negative microorganisms [4-7]. However, as a strong oxidant, the high concentration of eugenol caused the increased generation of tissue-damaging free radicals, resulting in the inflammatory and allergic reactions because of the formation of phenoxyl radicals and quinone intermediate. According to the Food and Agriculture Organization (FAO) and the World Health Organization (WHO), an acceptable daily intake of eugenol is  $2.5 \text{ mg kg}^{-1}$  [8]. Thus, it is necessary to construct a much more sensitive method for the detection of eugenol in our daily life.

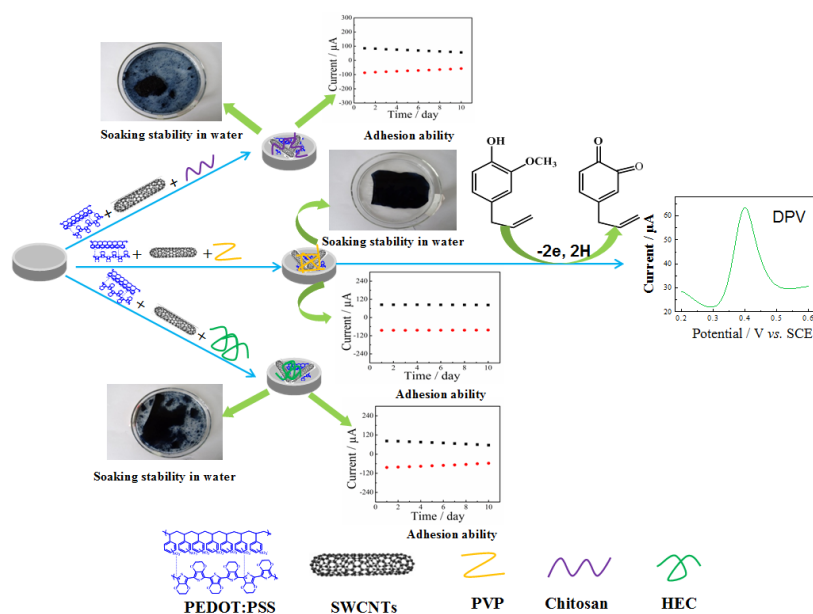
Up to now, various analytical technologies have been employed for the determination of eugenol in real samples, such as high performance liquid chromatography (HPLC), gas chromatography-mass spectrometry, liquid chromatography-mass spectrometry, and high-resolution mass spectrometry [9-12]. In comparison to these conventional methods, electrochemical analysis methods have certain advantages for the detection of eugenol owing to its fast analysis, low cost, high sensitivity, miniaturization, and simplicity. Moreover, the modifications of bare electrodes suffer remarkable advantages during the design and construct of electrochemical sensors [13]. In operation, the modified layers shuttle electrons between analytes in solutions and bare electrodes, which can accelerate electron transfer reaction and significantly reduce the over-potential. Moreover, compared to bare electrodes, the chemically modified electrodes are less susceptible to surface fouling and oxide formation. In addition, electrode modification has been employed as an effective approach to improve the sensitivity and enhance reproducibility. Different chemically modified electrodes like poly(diallyldimethylammonium chloride) functionalized graphene-MoS<sub>2</sub>, nanoCu doped gold nanoparticles, gold nanoparticles, and TiO<sub>2</sub> nanotubes incorporated with Cu<sub>2</sub>O clusters, have hitherto been developed for the determination of eugenol [14-17]. However, to the best of our knowledge, there are no reports on electronically conducting polymers (ECPs) as chemically modified electrodes for eugenol sensing.

Poly(3,4-ethylenedioxythiophene):poly(4-styrenesulfonate) (PEDOT:PSS) is a water dispersible form of the intrinsically conducting PEDOT polymer, which is quite promising attributing to its enormous advantages over other ECPs, especially solution processability, miscibility, mechanical flexibility, mass production, high transparency and tunable electrical conductivity, which is today the most successful ECPs, and has been produced commercially on a large-scale and sold for different application in academic and industrial fields [18]. In these PEDOT:PSS dispersions, PEDOT is charge transporting species and carries positive charges, while PSS acts as a charge-compensating counter polyanion and charge-balancing dopant to stabilize PEDOT and form a processable water-borne dispersion of negatively charged swollen colloidal particles consisting of both PEDOT and excess PSS [19]. Moreover, The preparation cost of PEDOT:PSS electrode could be reduced by mass production with conventional solution processing. Thus, PEDOT:PSS is quite promising as a next-generation transparent organic electrode material because of its enormous advantages over other ECPs. It can be used as an alternative to ITO in the development of a flexible, transparent and conducting electrode for various application in optical devices, electronic device, and optoelectronic devices, especially in organic photovoltaic devices, organic light-emitting diodes, and polymer field-effect transistors. Unfortunately, it is extremely easy to swell, disintegrate and crack when PEDOT:PSS film immerses

in aqueous solution, even become much more easily peel off from the surface of substrate electrode due to the relatively poor adhesion force between PEDOT:PSS layer and the surface of substrate electrode, which limited potential application of PEDOT:PSS film electrode in different devices like sensors, transistor, capacitors, cells, and batteries, only few reports on PEDOT:PSS film electrode as novel sensing materials for the application of chemo/bio-sensors. Hence, a highly water-stable and adhesive PEDOT:PSS film electrode is needed.

Different enhanced materials like ionic liquids, bis(fluorinated phenyl azide), multivalent cations, Nafion, zinc oxide (ZnO) rods, and poly(vinyl alcohol) was selected for the preparation and sensing application of highly water-stable and adhesive PEDOT:PSS film electrodes [20-25]. In addition, PEDOT:PSS derivatives also designed and synthesized for sensing application of high-performance PEDOT:PSS film electrodes [25], Moreover, different methods and combinatorial methods such as ionic cross-linking [21], the physical crosslinking [26], and electrochemical doping [22], have been proposed to improve the aforementioned problems. The as-obtained high-performance PEDOT:PSS electrodes have been employed as the electrode material for electrochemical application in bio/chemo sensors.

Since discovered by Iijima in 1991 [27], carbon nanotubes (CNTs) have been widely used for the divers sensing application due to its outstanding properties [28]. With the advantage of minimizing fouling of electrode surfaces, CNTs exhibited an excellent ability to enhance electrocatalytic activity, accelerate the electron transfer between electroactive species and electrodes, and increase specific surface area [29-30]. Moreover, the formation of CNTs/polymer composites has been explored for possible improvement in the electrocatalytic, electrical, and chemical properties of polymers [31]. Among them, the electrochemical sensors based on ECPs and hybrid composite of CNTs have received significant interest because the synergistic effect of composite materials.



**Scheme 1.** The fabrication process, soaking stability in water, and adhesion stability of three different PEDOT:PSS composite film electrodes, and the working mechanism and practical sample analysis of eugenol at PEDOT:PSS-SWCNTs-PVP/GCE.

Inspired by these aspects, three common polymeric materials, such as chitosan, hydroxyethyl cellulose (HEC) and polyvinylpyrrolidone (PVP) with good film-forming and adhesive properties, high tensile strength, and hypotoxicity, as binders and stabilizers were incorporated into the mixed aqueous solution of PEDOT:PSS and single-walled carbon nanotube (SWCNTs), respectively. Three PEDOT:PSS composite electrodes were prepared by drop-coating the corresponding mixed solution on the surface of glassy carbon electrode (GCE). The high-performance PEDOT:PSS-SWCNTs-PVP/GCE was successfully employed for the highly sensitive determination of eugenol in food samples (Scheme 1).

## 2. EXPERIMENTAL

### 2.1 Chemicals

PEDOT:PSS aqueous dispersion (1.3 wt%) was obtained from Bayer AG. SWCNTs suspension (1.0 wt%) was provided from Nanjing XFNANO Materials Tech Co., Ltd. Eugenol, chitosan, HEC and PVP were obtained from J&K Scientific Ltd. 0.1 M phosphate buffer solutions (PBS) with different pH values were prepared from stock solutions of 0.1 M  $\text{H}_3\text{PO}_4$ ,  $\text{NaH}_2\text{PO}_4$ ,  $\text{Na}_2\text{HPO}_4$ , and NaOH. Double-distilled water was employed throughout the experiments. All reagents were analytical grade.

### 2.2 Instrument

All the electrochemical measurements were performed in a conventional three-electrode system with a CHI660B electrochemical workstation (Shanghai Chenhua Instrument Co., China). The conventional three-electrode cell system included a glassy carbon electrode (GCE) ( $\Phi = 3$  mm) as the working electrode, Pt wire ( $\Phi = 1$  mm) as the auxiliary electrode and a saturated calomel electrode (SCE) as the reference electrode. The counter electrode was carefully polished with abrasive paper (1500 mesh), cleaned successively with water and acetone, and then dried in air before each experiment. The bare GCE was polished with alumina ( $\text{Al}_2\text{O}_3$ , 0.05  $\mu\text{m}$ ), rinsed with double-distilled water and cleaned ultrasonically, and then dried at room temperature. Electrochemical impedance spectroscopy was performed in 5 mM  $\text{K}_3\text{Fe}(\text{CN})_6/\text{K}_4\text{Fe}(\text{CN})_6$  (1:1) mixture with 0.1 M KCl at the formal potential of the 180 mV using alternating voltage of 5 mV. The frequency range was from 0.1 Hz to 10 kHz. Prior to each experiment, all solutions were deoxygenated by bubbling with dry argon for 10 min.

### 2.3 Preparation of three composite modified electrodes

Chitosan (2 wt%), HEC (2 wt%) and PVP (2 wt%) were mixed using PEDOT:PSS (1.3 wt%) aqueous solution in the volume rate of 9:1 in order to improve the water stability of PEDOT:PSS film, and then stirred thoroughly for 24 h at room temperature, respectively. Subsequently, SWCNTs

suspension (1.0 wt%) was added into PEDOT:PSS-chitosan, PEDOT:PSS:PSS-HEC and PEDOT:PSS-PVP aqueous dispersions in the volume rate of 8:1 and stirred thoroughly for 24 h at room temperature, respectively. The PEDOT:PSS-SWCNTs-chitosan/GCE, PEDOT:PSS-SWCNTs-HEC/GCE and PEDOT:PSS-SWCNTs-PVP/GCE were obtained by drop-coating 5  $\mu$ L PEDOT:PSS-SWCNTs-chitosan, PEDOT:PSS-SWCNTs-HEC and PEDOT:PSS-SWCNTs-PVP mixed suspensions on the bare GCE surfaces respectively, and dried at room temperature.

#### 2.4 Analytical procedure

0.1 M pH 6.0 PBS was used as supporting electrolyte. Five milliliters of PBS with a specific amount of eugenol solution was transferred into the sealed electrochemical cell by microsyringe. The modified electrodes were immersed into a stirring 0.1 M PBS containing the desired concentration of eugenol for 200 s. Differential pulse voltammetry (DPV) curves were recorded from 0 to 0.8 V vs. SCE, and the anodic peak currents were measured. The DPV conditions were as follows: potential increase of 0.004 V, amplitude of 0.05 V, pulse width of 0.05 s and pulse interval of 0.2 s.

### 3. RESULTS AND DISCUSSION

#### 3.1 Flexibility and soaking stability

The surface of PEDOT:PSS-SWCNTs-PVP film was smooth and easily bended or twisted without cracking (Fig. 1 (A1-A2)).

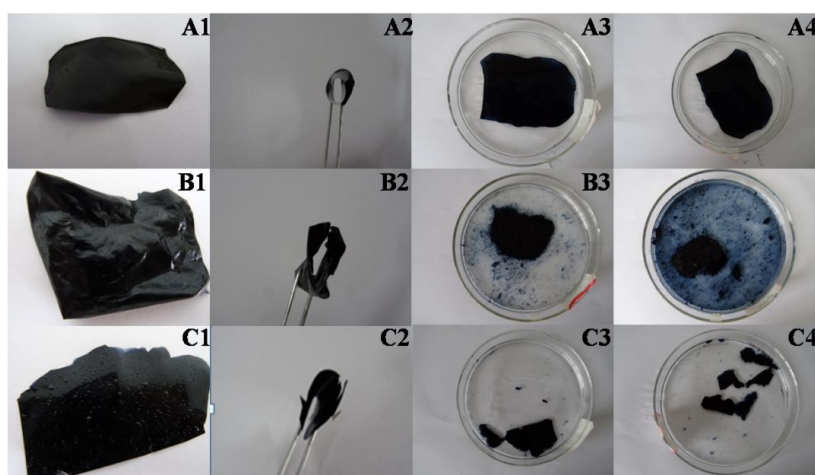


**Figure 1.** The surface topography of PEDOT:PSS-SWCNTs-chitosan film (A1), PEDOT:PSS-SWCNTs-HEC film (B1) and PEDOT:PSS-SWCNTs-PVP film (C1); the flexibility of PEDOT:PSS-SWCNTs-chitosan film (A2), PEDOT:PSS-SWCNTs-HEC film (B2) and PEDOT:PSS-SWCNTs-PVP film (C2); the soaking stability of PEDOT:PSS-SWCNTs-chitosan film (A(3-4)), PEDOT:PSS-SWCNTs-HEC film (B(3-4)) and PEDOT:PSS-SWCNTs-PVP film (C(3-4)) in water for 5 days and 10 days, respectively.

Although the surface of PEDOT:PSS-SWCNTs-chitosan film appeared many wrinkles, the composite film still exhibited good flexibility when this film was rolled up (Fig. 1 (B1-B2)). As can be seen from Fig. 1(C1), the surface of PEDOT:PSS-SWCNTs-HEC film was found to be irregular, and many small protuberances were distributed on the film. It also had a strong flexibility after bent (Fig. 1 (C2)). Three composite films were immersed into double-distilled water to observe the changes of their soaking stability. PEDOT:PSS-SWCNTs-PVP film exhibit highly soaking stability even after immersion in water for 5 and 10 days, respectively (Fig. 1 (A3-A4)). For PEDOT:PSS-SWCNTs-chitosan film, its edge began to swell and disintegrate after immersion in water for 5 days (Fig. 1 (B3)). After immersion in water for 10 days, about 30% PEDOT:PSS-SWCNTs-chitosan film was lost (Fig. 1(B4)). PEDOT:PSS-SWCNTs-HEC film occur a few cracks and fragments after immersion in water for 5 days (Fig. 1(C3)). After 10 days, PEDOT:PSS-SWCNTs-HEC film disintegrate more fragments (Fig. 1(C4)). PEDOT:PSS-SWCNTs-PVP film demonstrated best soaking stability in comparison with PEDOT:PSS-SWCNTs-chitosan film and PEDOT:PSS-SWCNTs-HEC film.

### 3.2 Adhesion stability

To study the adhesion stability of PEDOT:PSS-SWCNTs-chitosan film, PEDOT:PSS-SWCNTs-HEC film, and PEDOT:PSS-SWCNTs-PVP film toward the surface of bare GCE, the three composite electrodes were stored in  $[\text{Fe}(\text{CN})_6]^{3-/4-}$  solution for 10 days (Fig. 2), and the redox peak currents of  $[\text{Fe}(\text{CN})_6]^{3-/4-}$  for CVs were used to study the adhesion stability of these film electrodes.

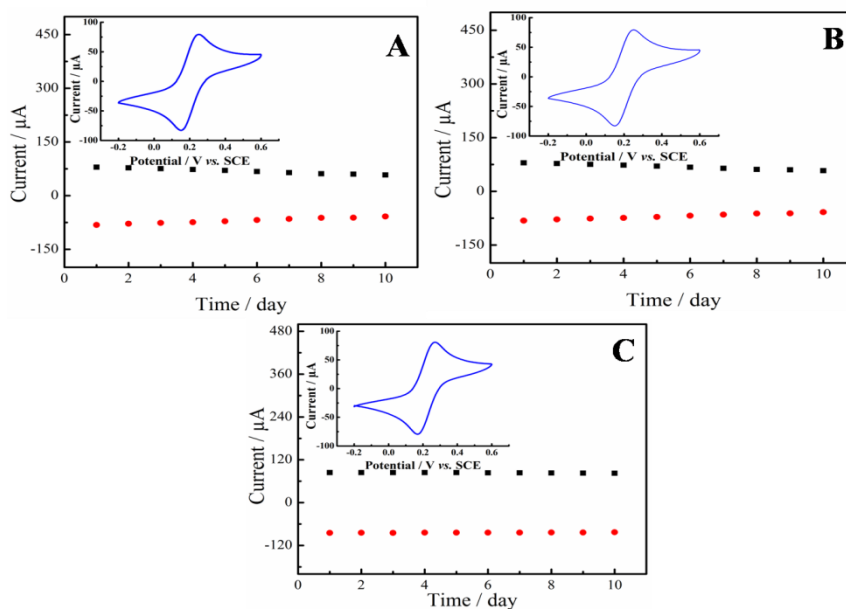


**Figure 2.** The adhesion stability of PEDOT:PSS-SWCNTs-chitosan/GCE (A), PEDOT:PSS-SWCNTs-HEC/GCE (B), and PEDOT:PSS-SWCNTs-PVP/GCE (C). Three different PEDOT:PSS composite film electrodes were analyzed periodically for 10 days in 10 mM  $[\text{Fe}(\text{CN})_6]^{3-/4-}$  solution containing 0.1 M KCl by using CVs. Insets: CV curves of PEDOT:PSS-SWCNTs-chitosan/GCE (A), PEDOT:PSS-SWCNTs-HEC/GCE (B), and PEDOT:PSS-SWCNTs-PVP/GCE (C), respectively.

Under the same conditions, the tests were carried out every day and continuously for 10 days. The relative standard deviations (RSDs) of two redox current peaks for  $[\text{Fe}(\text{CN})_6]^{3-/4-}$  on PEDOT:PSS-SWCNTs-chitosan/GCE were 13.6% and 11.1%, respectively (Fig. 2A). With PEDOT:PSS-SWCNTs-HEC/GCE, the RSDs of redox current peaks were 12.7% and 9.2%, respectively (Fig. 2B). For PEDOT:PSS-SWCNTs-PVP/GCE, RSDs of redox current peaks were 3.6% and 2.1%, respectively (Fig. 2C). These results indicated that PEDOT:PSS-SWCNTs-PVP/GCE had best adhesive stability than PEDOT:PSS-SWCNTs-chitosan/GCE and PEDOT:PSS-SWCNTs-HEC/GCE.

### 3.3 Cycle stability

The long-term cycle stability of three composite electrodes were investigated by performing 500 cycles of CV tests with the potential range of 0.2–0.8 V at a sweep rate of 50  $\text{mV s}^{-1}$  in 0.1 M PBS (Fig. 3). The specific capacitance ( $C_s$ ) was estimated from CVs using Equation (1):

$$C_s = \frac{\int_{E_1}^{E_2} i(E) dE}{2vm(E_2 - E_1)} \quad \text{Equation (1)}$$

Where  $E_1$  and  $E_2$  are the cutoff potentials in CV,  $i(E)$  is the instantaneous current,  $i(E)dE$  is the total voltammetric charge obtained by integration of the positive and negative sweeps in the CVs,  $v$  is the scan rate, and  $m$  is the mass of the individual sample. After 500 cycles, the  $C_s$  of PEDOT:PSS-SWCNTs-chitosan/GCE and PEDOT:PSS-SWCNTs-HEC/GCE decreased by 22.4% and 25.7% of the initial  $C_s$ , respectively (Fig. 3(A-B)).

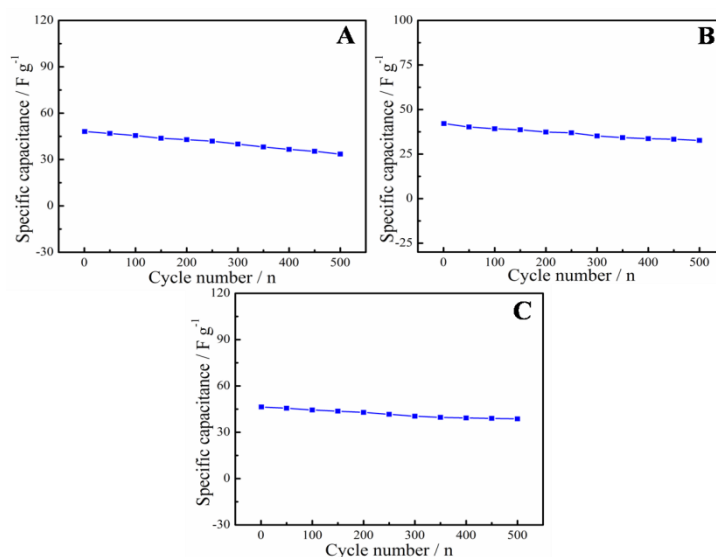


**Figure 3.** Cycle stability of the specific capacitance of the electrode materials using PEDOT:PSS-SWCNTs-chitosan (A), PEDOT:PSS-SWCNTs-HEC (B), and PEDOT:PSS-SWCNTs-PVP (C) as electrode active materials, respectively.

In comparison with that of PEDOT:PSS-SWCNTs-chitosan/GCE and PEDOT:PSS-SWCNTs-HEC/GCE, the cycle stabilities of PEDOT:PSS-SWCNTs-PVP/GCE increased, and its  $C_s$  remained at

88.3% of the initial  $C_s$  after 500 cycles (Fig. 3C). The result indicated that PEDOT:PSS-SWCNTs-PVP/GCE had better cycle stability than other two electrodes which also further implied that introduction of PVP enhanced stability in water, and delayed the swelling, disintegration, cracking and peeling-off of PEDOT:PSS film in water.

### 3.4 Conducting property

Electrochemical impedance spectroscopy of the modified electrodes are shown in Fig. 4. Obviously, the bare GCE (curve a) exhibited a semicircle portion and the value of electron-transfer resistance ( $R_{et}$ ) was estimated to be 272.6  $\Omega$  (curve a). The  $R_{et}$  of PEDOT:PSS-SWCNTs-chitosan/GCE was 6.2  $\Omega$  (curve b). After drop-coating PEDOT:PSS-SWCNTs-HEC/GCE onto the surface of bare GCE, its  $R_{et}$  was decreased to 6.2  $\Omega$  (curve c). The  $R_{et}$  value of PEDOT:PSS-SWCNTs-PVP/GCE was 3.1  $\Omega$  (curve d). This decrease is probably owing to the better electrical conductivity of PVP than chitosan and HEC.

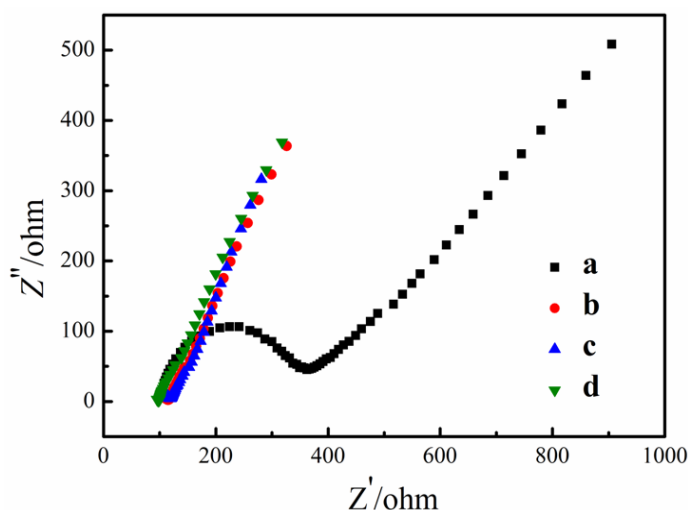


**Figure 4.** Nyquist plots of bare GCE (a), PEDOT:PSS-SWCNTs-chitosan/GCE (b), PEDOT:PSS-SWCNTs-HEC/GCE (c), and PEDOT:PSS-SWCNTs-PVP/GCE (d) in 10 mM  $[\text{Fe}(\text{CN})_6]^{4-/3-}$  solution containing 0.1 M KCl.

### 3.5 Electrochemical behaviors of eugenol

For the first scan of CVs (Fig. 5A), only one oxidation reaction (anodic peak a,  $E_a = 0.41$  V) corresponding to the formation of one electroactive product was observed [14]. The reverse scan of the first CV appeared peak b (cathodic peak b,  $E_b = 0.12$  V), corresponding to the reduction of the eugenol oxidation product formed after the eugenol oxidation in the first cycle. In the second and third scans, a new anodic peak c (anodic peak c,  $E_c = 0.172$  V) appeared, and peak currents of the current profiles b and c were very similar, demonstrating that anodic peak b and cathodic peak c were reversible, which displayed a similar voltammetric feature of previous reported literature [15].

The electrochemical behaviors of eugenol based on bare GCE (curve a) SWCNT/GCE (curve b), PEDOT:PSS-SWCNTs-chitosan/GCE (curve c), PEDOT:PSS-SWCNTs-HEC/GCE (curve d) and PEDOT:PSS-SWCNTs-PVP/GCE (curve e) were studied by second scan of CVs in PBS (pH 6.0) with a scan rate of  $50 \text{ mV s}^{-1}$  (Fig. 5B). Only a weak and broad anodic peak (0.51 V) and a very poor cathodic peak (0.08 V) were appeared at the bare GCE (curve a). A pair of well-defined redox peaks and an irreversible anode peak was observed at SWCNT/GCE, which attributed to large surface area, fast electron transfer and excellent electrocatalytic activity of SWCNTs [30]. Compared with SWCNTs/GCE, a remarkable increase in peak currents and negative shift of anodic peak potential were shown at PEDOT:PSS-SWCNTs-chitosan/GCE, PEDOT:PSS-SWCNTs-HEC/GCE and PEDOT:PSS-SWCNTs-PVP/GCE, respectively, which attributed to the synergistic enhanced effect of different components. The ECPs act as conductive bridges to connect the isolated SWCNTs regions, resulting in the increased conductivity; the SWCNTs plays the role of a electro-active site to increase the velocity of electron transfer for the redox of eugenol and enhance the 2D conducting properties for the hybrid material [31]. Moreover, the oxidation current of eugenol was greatly increased and the peak potential for eugenol had shift negatively on PEDOT:PSS-SWCNTs-PVP/GCE in compared with PEDOT:PSS-SWCNTs-chitosan/GCE and PEDOT:PSS-SWCNTs-HEC/GCE. The obvious peak current enlargements indicated that PEDOT:PSS-SWCNTs-PVP/GCE had most active to the electrochemical oxidation of eugenol, might be attributed to the high accumulation efficiency of PVP with hydrophobic backbone and heterocyclic groups [32]. Therefore, PEDOT:PSS-SWCNTs-PVP/GCE was employed to detect eugenol in the subsequent experiment.

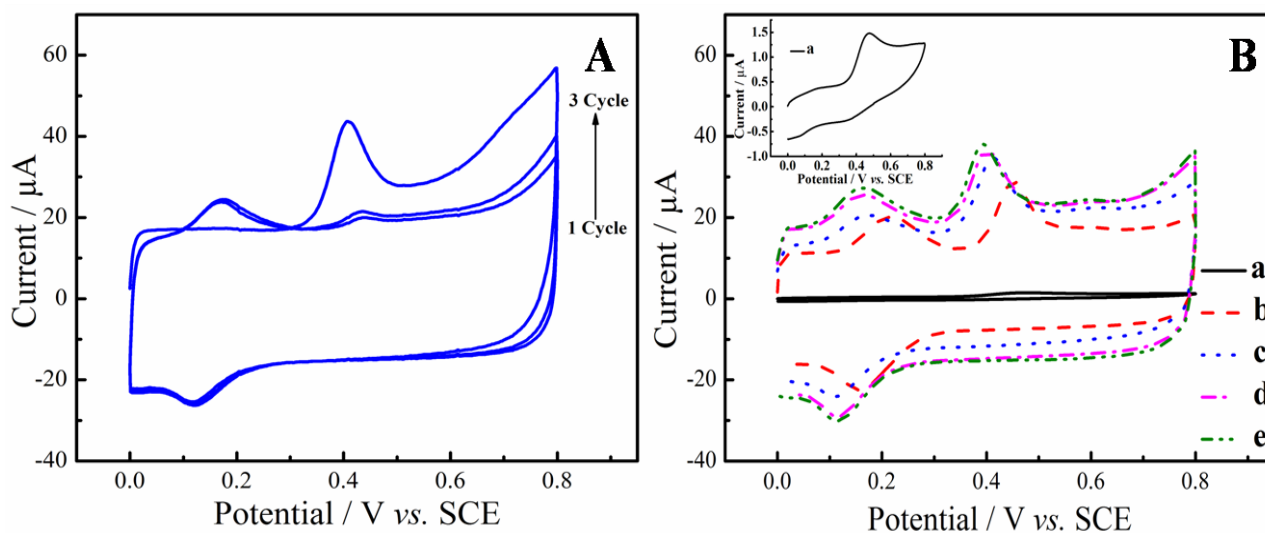


**Figure 5.** Consecutive CVs of eugenol at PEDOT:PSS-SWCNTs-PVP/GCE in PBS (pH 6.0) with a scan rate of  $50 \text{ mV s}^{-1}$ , CVs (B) of bare GCE (a), SWCNTs/GCE (b), PEDOT:PSS-SWCNTs-chitosan/GCE (c), PEDOT:PSS-SWCNTs-HEC/GCE (d), and PEDOT:PSS-SWCNTs-PVP/GCE (e) in 0.1 M PBS (pH 6.0) containing  $50 \text{ μM}$  eugenol.

### 3.6 Optimization of experimental conditions

#### 3.6.1 Effect of scan rates

The effect of scan rates ( $\nu$ ) on electrochemical behaviors of eugenol with a constant concentration (50  $\mu\text{M}$ ) at PEDOT:PSS-SWCNTs-PVP/GCE was investigated by CVs with the potential range of 0.2-0.8 V (Fig. 6A). The three peak currents clearly enhanced with the increasing  $\nu$  from 10 to 200  $\text{mV s}^{-1}$ . Moreover, the peak currents ( $I_a$ ,  $I_b$ , and  $I_c$ ) were proportional to  $\nu$ , confirming that the electrochemical behaviors of eugenol were adsorption-controlled electrode processes (Fig. 6B). In addition, the anodic peak potential at the first anodic sweep ( $E_a$ ) shifted linearly with changed in the Napierian logarithm of scan rates ( $\ln \nu$ ) (Fig. 6C). According to Laviron theory [33], the relationship between peak potentials and scan rates is:

$$E_{\text{pa}} = E^0 + \frac{RT}{\alpha nF} \ln \frac{RTK_s}{\alpha nF} - \frac{RT}{\alpha nF} \ln \nu \quad \text{Equation (2)}$$

$$E_{\text{pc}} = E^0 + \frac{RT}{(1-\alpha)nF} \ln \left[ \frac{RTK_s}{(1-\alpha)nF} \right] - \frac{RT}{(1-\alpha)nF} \ln \nu \quad \text{Equation (3)}$$

$E^0$  refers to the formal standard potential,  $\alpha$  is charge transfer coefficient;  $n$  is the number of the electrons transferred involved in the electrode reaction. Other symbols have their usual meanings. From the slope,  $\alpha n$  is calculated to be 0.8, assuming  $\alpha$  is 0.5 in a totally irreversible electrode process. Thus,  $n$  is approximately to 2, implying that two electron is involved in the oxidation of eugenol.

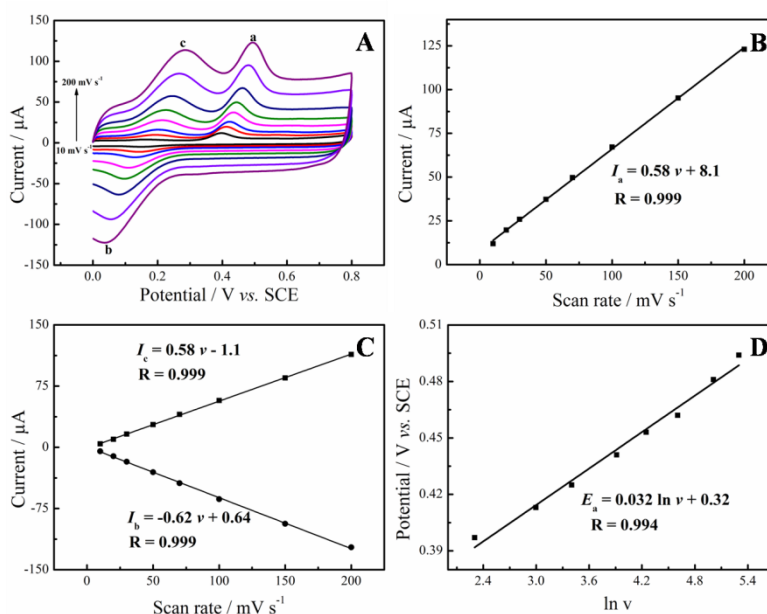


**Figure 6.** CVs (A) of 50  $\mu\text{M}$  eugenol at PEDOT:PSS-SWCNTs-PVP/GCE in 0.1 M PBS (pH 6.0) with different scan rates: 10, 20, 30, 50, 70, 100, 150, and 200  $\text{mV s}^{-1}$ . The plots of  $I_a$  (B),  $I_b$  and  $I_c$  (C) vs.  $\nu$  at PEDOT:PSS-SWCNTs-PVP/GCE; The plots (D) of  $E_a$  vs.  $\ln \nu$  at PEDOT:PSS-SWCNTs-PVP/GCE.

### 3.6.2 Effect of pH

The effect of pH values on the determination of eugenol using PEDOT:PSS-SWCNTs-PVP/GCE were investigated over the pH range from 5.0 to 7.0. With the increasing pH of the solution, the  $I_a$  of eugenol increased gradually, and achieved a maximum at about pH 6.0, then the  $I_a$  decreased with the further increasing of pH values. Therefore, pH 6.0 of 0.1 M PBS was selected for the analysis of eugenol at PEDOT:PSS-SWCNTs-PVP/GCE (Fig. 7).

With the increasing of pH value, the  $E_a$  shifted negatively, indicating that protons have taken part in the electrode oxidation process of eugenol. The plots  $E_a$  vs pH was attained and gave straight lines with a slope of -0.045 at PEDOT:PSS-SWCNTs-PVP/GCE. According to the Nernst equation [34],

$$dE_{pa}/dpH = (-2.303mRT)/nF \quad \text{Equation (4)}$$

$m$  and  $n$  is the number of protons and electrons involved in the electrochemical reaction, and  $R$ ,  $T$  and  $F$  have their usual meanings. The value of  $m/n$  can be calculated according to the slope of  $E_{pa}$  versus pH. The ratio of  $m/n$  was approximately to 1, suggesting that the number of electrons and protons were equal. Therefore, the electrochemical oxidation process of eugenol should be two electrons and two protons, which was also consistent with previously reported results [15].

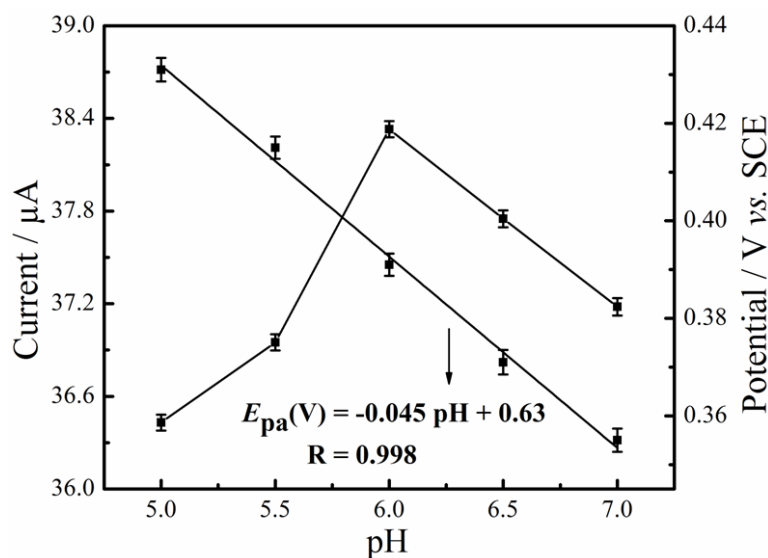


**Figure 7.** Effect of pH on peak currents and peak potentials of eugenol oxidation at PEDOT:PSS-SWCNTs-PVP/GCE.

### 3.6.3 Effect of accumulation time

To assess the influence of accumulation potential and accumulation time, the  $I_a$  of 50  $\mu\text{M}$  eugenol at PEDOT:PSS-SWCNTs-PVP/GCE were measured under different accumulation potentials and accumulation times, respectively. The accumulation potential results showed that the anodic peak currents changed slightly, implying that accumulation potential had no almost influence. Thus, the initial potential was performed for the sake of convenience. As shown in Fig. 8, the peak current

increased rapidly with the increasing of accumulation time, and reached a platform at 200 s, and then kept constant when accumulation times extended from 200 to 300 s. Therefore, the accumulation time of 200 s was selected for further studies.

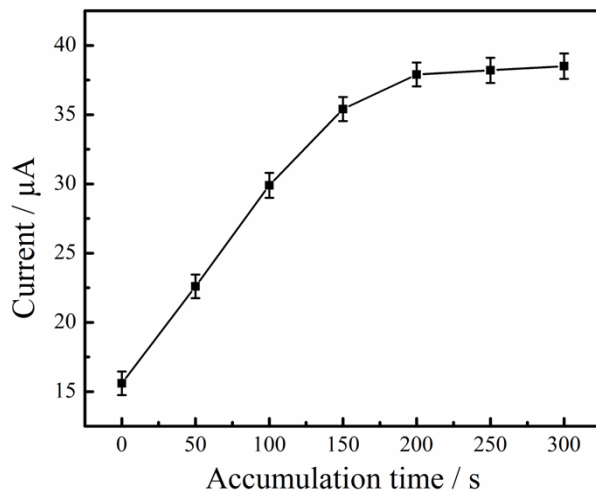
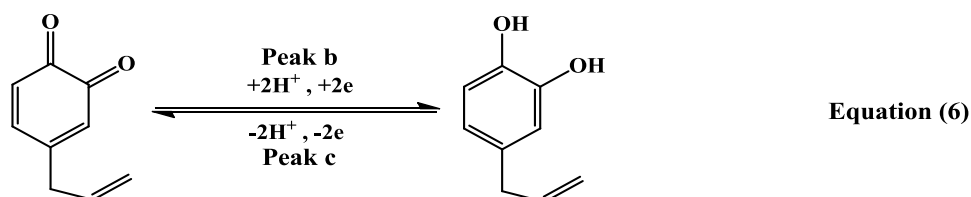
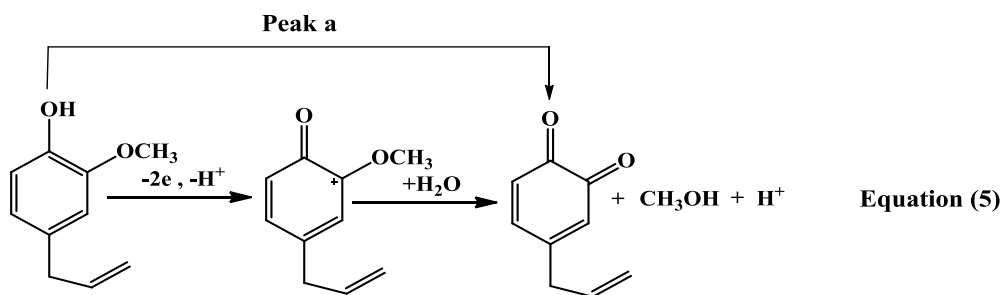


**Figure 8.** Effect of preconcentration time on voltammetric responses of eugenol at PEDOT:PSS-SWCNTs-PVP/GCE in 0.1 M PBS (pH 6.0) containing 50 μM eugenol.

### 3.7 Electrochemical reaction mechanism of eugenol

In previous reported literatures [15], the electrochemical behaviors of eugenol showed two anode peaks (peak a and c) and a single cathode peak (peak b). The first anode peak (peak a) corresponded to the oxidation of hydroxy and hydroxymethyl groups to ketone groups via a two-electron oxidation process (Equation (5)). The reversible redox peaks were attributed to two-electron transfer on two ketone species transform to hydroxy groups (Equation (6)).



3.8 Analytical performance

3.8.1 Electrochemical determination of eugenol

PEDOT:PSS-SWCNTs-PVP/GCE displayed extraordinary electrochemical behaviors for the oxidation of eugenol. DPV, as a sensitive and low detection limit electrochemical method, was used to investigate the relationship between the current responses and eugenol concentrations under optimal conditions of the prepared electrochemical sensor.

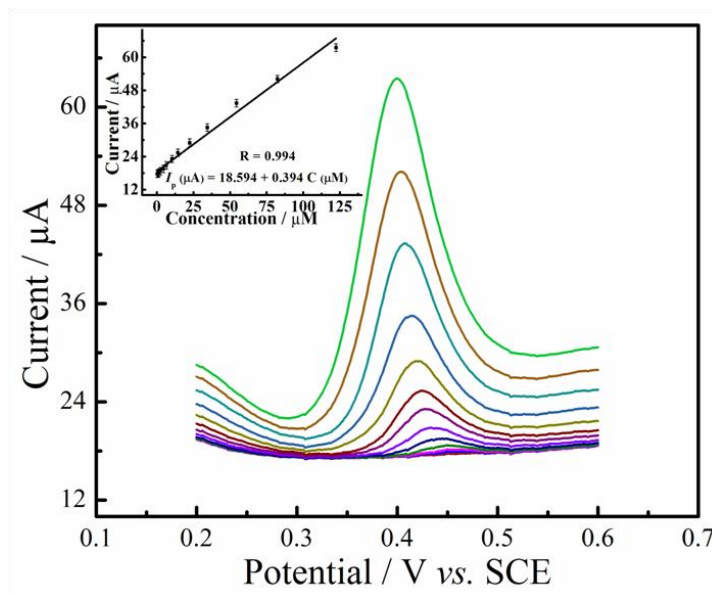


**Figure 9.** DPV responses of eugenol with various concentrations at PEDOT:PSS-SWCNTs-PVP/GCE; Inset: the calibration plots of eugenol.

**Table 1.** The comparison of electrochemical sensing performance using other previously reported sensing electrodes for the determination of eugenol.

Electrode	Buffer solution	Linear range (µM)	Limit of detection (µM)	Reference
Au/PDDA-G-MoS <sub>2</sub> /GCE	NaAc-HAc (pH 5.5)	0.1-440	0.036	[19]
AuNPs modified carbon paste electrode	PBS (pH 8.0)	5.0-250	2.0	[20]
Cu <sub>2</sub> O-TiNTs/GCE	NaClO <sub>4</sub> /Acetonitrile (pH 7.0)	4.6-450	1.3	[21]
Cu@AuNPs/GCE/GCE	BR (pH 2.0)	0.3-4.9	0.25	[22]
PEDOT:PSS-SWCNTs-PVP/GCE	PBS (pH 6.0)	0.15-122.4	0.048	This work

Fig. 9 showed DPV responses of eugenol at different concentrations using PEDOT:PSS-SWCNTs-PVP/GCE, and peak currents were proportional to the concentrations of eugenol.

PEDOT:PSS-SWCNTs-PVP/GCE showed a linear range from 0.15-122.4  $\mu\text{M}$  with a low detection limit ( $LOD$ ) of 0.048  $\mu\text{M}$  ( $S/N = 3$ ). Moreover, a comparison analysis on eugenol electrochemical sensors based on different modified electrodes reported in the literature was listed in Table 1. This results indicated that the fabricated electrochemical sensor displayed the better sensing performance compared with the reported sensors.

### 3.8.2 Repeatability, long-term stability and interference

The reproducibility of prepared electrochemical sensor was studied by repeating detection the certain concentration of eugenol. RSD was 3.1% for 20 parallel measurements, suggesting the remarkable reproducibility and precision of composite modified electrodes (Fig. 10). After stored for 15 days at 4  $^{\circ}\text{C}$  in refrigerator, approximately 98.4% of its original response was remained, suggesting the good long-term stability of composite modified electrodes.

The interferences of common inorganic ion, some saccharine and organic compounds were evaluated at the PEDOT:PSS-SWCNTs-PVP/GCE for the determination of eugenol. The responses of the modified electrode to 2  $\mu\text{M}$  eugenol were not affected by additions of 1000-fold concentration of sucrose, glucose, glycine and lactose, and 100-fold concentration of  $\text{Na}^+$ ,  $\text{K}^+$ ,  $\text{Ca}^{2+}$ ,  $\text{Zn}^+$ ,  $\text{Mg}^{2+}$ ,  $\text{NO}_3^-$ ,  $\text{Cl}^-$ ,  $\text{CO}_3^-$  and  $\text{SO}_4^{2-}$ , and 10-fold concentration of amaranth, tartrazine, and tryptophan.

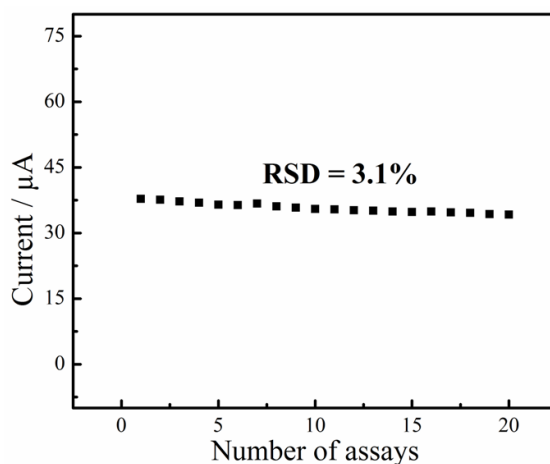


**Figure 10.** The operational stability for the voltammetric detection of eugenol at PEDOT:PSS-SWCNTs-PVP/GCE.

### 3.8.3 Analytical application in real samples

The fabricated electrode was implemented to determine the eugenol in curry powder samples to evaluate the validity of the proposed method by using the standard addition method, as listed in Table 2. The recoveries of eugenol were in the range of 98.3–102.5%, and the RSDs were all below 3%. In order to confirm the accuracy of the as-fabricated sensor based on PEDOT:PSS-SWCNTs-PVP/GCE, the same content of eugenol was also detected using HPLC. The results obtained by HPLC were in good agreement with that obtained by the as-fabricated sensor based on PEDOT:PSS-SWCNTs-

PVP/GCE, suggesting the accurate and feasible of this method. Thus, this sensor could be employed for the simple and efficient determination of eugenol in our daily life.

**Table 2.** The determination and recoveries of eugenol in curry powder sample at the PEDOT:PSS-SWCNTs-PVP/GCE.

Electrode	Added ( $\mu\text{M}$ )	Found <sup>a</sup> ( $\mu\text{M}$ )	Recovery (%)	RSD (%)	Determined by HPLC <sup>a</sup> ( $\mu\text{M}$ )
PEDOT:PSS-SWCNTs-PVP/GCE	—	10.51 $\pm$ 0.16	—	2.02	10.62 $\pm$ 0.14
	20.00	26.56 $\pm$ 0.21	102.5	1.96	26.68 $\pm$ 0.15
	40.00	44.83 $\pm$ 0.24	98.3	2.15	44.74 $\pm$ 0.17
	80.00	61.12 $\pm$ 0.16	100.9	1.89	60.97 $\pm$ 0.15

#### 4. CONCLUSION

Three flexible PEDOT:PSS composite film such as PEDOT:PSS-SWCNTs -chitosan, PEDOT:PSS-SWCNTs-HEC and PEDOT:PSS-SWCNTs-PVP were prepared and characterized. PEDOT:PSS-SWCNTs-PVP exhibited most excellent performance in soaking stability, adhesive ability, cyclic stability, conductivity and electrocatalytic activity. Moreover, PEDOT:PSS-SWCNTs-PVP/GCE could successfully realized for the detection of eugenol in food samples, satisfactory results indicated that PEDOT:PSS-SWCNTs-PVP/GCE with electrode stability in water will provide a promising platform for the potential application of various devices in water.

#### ACKNOWLEDGEMENTS

The authors would like to acknowledge the financial support of this work by the National Natural Science Foundation of China (51463008), Jiangxi Provincial Department of Education (GJJ14301), Ganpo Outstanding Talents 555 projects (2013), Training Plan for the Main Subject of Academic Leaders of Jiangxi Province, and Youth Science and Technology Talent Training Plan of Chongqing Science and Technology Commission (CSTC2014KJRC-QNRC10006).

#### References

1. E.Y. Backheet, *Phytochem. Anal.*, 9 (1998) 134.
2. K. Schulz, K. Schlenz, S. Malt, R. Metasch, W. Römhild, and J. Dreßler, *J. Chromatogr. A*, 1211 (2008) 113.
3. V. V. Dighe, A. A. Gursale, R. T. Sane, S. Menon, and P. H. Patel, *Chromatographia*, 61 (2005) 443.
4. Y. Irie, and W. M. Keung, *Brain Res.*, 963 (2003) 282.

5. K. H. Son, S. Y. Kwon, H. P. Kim, H. W. Chang, and S. S. Kang, *Nat. Prod. Sci.*, 4 (1998) 263.
6. H. C. Ou, F. P. Chou, T. M. Lin, C. H. Yang, and W. H. Sheu, *Food Chem. Toxicol.*, 44 (2006) 1485.
7. D. Kalemba, and A. Kunicka, *Curr. Med. Chem.*, 10 (2003) 813.
8. G. Dhoot, R. Auras, M. Rubino, K. Dolan, and H. Soto-Valdez, *Polymer*, 50 (2009) 1470.
9. G. M. Polzin, S. B. Stanfill, C. R. Brown, D. L. Ashley, and C. H. Watson, *Food Chem. Toxicol.*, 45 (2007) 1948.
10. F. Beaudry, S. A. Guenette, and P. Vachon, *Biomed. Chromatogr.*, 20 (2006) 1216.
11. C. L. Gopu, S. Aher, H. Mehta, A. R. Paradkar, and K. R. Mahadik, *Phytochem. Anal.*, 19 (2008) 116.
12. R. N. Goyal, V. K. Gupta, and S. Chatterjee, *Biosens. Bioelectron.*, 24 (2009) 3562.
13. A. A. Ensafi, M. Taei, and T. Khayamian, *J. Electroanal. Chem.*, 633 (2009) 212.
14. Q. L. Feng, K. Y. Duan, X. L. Ye, D. B. Lu, Y. L. Du, and C. M. Wang, *Sens. Actuators, B*, 192 (2014) 1.
15. X. Y. Lin, Y. N. Ni, and S. Kokot, *Electrochim. Acta*, 133 (2014) 484.
16. D. Afzali, S. Zarei, F. Fathirad, and A. Mostafavi, *Mater. Sci. Eng., C*, 43 (2014) 97.
17. S. Z. Kang, H. Liu, X. Q. Li, M. J. Sun, and J. Mu, *RSC Adv.*, 4 (2014) 538.
18. A. Elschner, S. Kirchmeyer, W. Lövenich, U. Merker, and K. Reuter, *PEDOT: Principles and Applications of an Intrinsically Conductive Polymer*, CRC Press Taylor & Francis Group, Boca Raton (2011).
19. M. Döbbelin, R. Marcilla, C. Tollan, J. A. Pomposo, J. R. Sarasua, and D. Mecerreyes, *J. Mater. Chem.*, 18 (2008) 5354.
20. G. Winroth, G. Latini, D. Credginton, L. Y. Wong, L. L. Chua, and P. K. H. Ho, *Appl. Phys. Lett.*, 92 (2008) 103308.
21. S. Ghosh, and O. Inganäs, *Synth. Met.*, 101 (1999) 413.
22. Y. Y. Yao, Y. P. Wen, L. Zhang, J. K. Xu, Z. F. Wang, and X. M. Duan, *Int. J. Electrochem. Sci.*, 8 (2013) 9348.
23. Z. F. Wang, J. K. Xu, Y. Y. Yao, L. Zhang, Y. P. Wen, H. J. Song, and D. H. Zhu, *Sens. Actuators, B*, 196 (2014) 357.
24. H. Zhang, J. K. Xu, Y. P. Wen, Z. F. Wang, J. Zhang, and W. C. Ding, *Synth. Met.*, 204 (2015) 39.
25. Z. F. Wang, Z. P. Wang, H. Zhang, X. M. Duan, J. K. Xu, and Y. P. Wen, *RSC Adv.*, 5 (2015) 12237.
26. S. Ghosh, J. Rasmusson, and O. Inganäs, *Adv. Mater.*, 10 (1998) 1097.
27. S. Iijima, *Nature*, 354 (1991) 56.
28. P. M. Ajayan, *Chem. Rev.*, 99 (1999) 1787.
29. T. Nie, L. M. Lu, L. Bai, J. K. Xu, K. X. Zhang, O. Zhang, Y. P. Wen, and L. P. Wu, *Int. J. Electrochem. Sci.*, 8 (2013) 7016.
30. M. Amadipour, M. A. Aher, H. Bitollahi, and R. Hseinzadehd, *Chin. Chem. Lett.*, 23 (2012) 981.
31. T. Y. Huang, C. W. Kung, H. Y. Wei, K. M. Boopathi, C. W. Chu, and K. C. Ho, *J. Mater. Chem. A*, 2 (2014) 7229.
32. X. F. Yang, and H. J. Zhang, *Food Chem.*, 102 (2007) 1223.
33. Laviron E, *J. Electroanal. Chem.*, 100 (1979) 263.
34. Z. F. Wang, H. Zhang, Z. P. Wang, J. Zhang, X. M. Duan, J. K. Xu, and Y. P. Wen, *Food Chem.*, 180 (2015) 186.